PROBABILITIES OF WESTERLY WIND BURSTS IN THE WESTERN EQUATORIAL PACIFIC, 1980-89

Leslie M. Hechtel
John A. Young

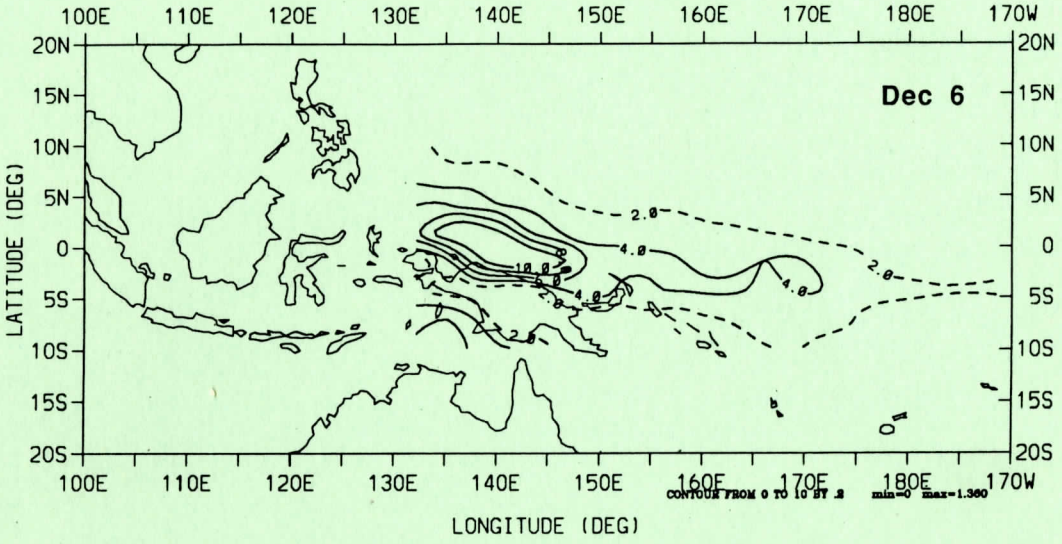

Department of Meteorology
University of Wisconsin - Madison
1225 West Dayton Street
Madison WI 53706

Scientific Report
National Science Foundation
Grant ATM87-17255
August 1991

CORRIGENDUM: All labeled and discussed probabilities in this report should be multiplied by 2.0. LMH and JAY, 1/92.

PROBABILITIES OF WESTERLY WIND BURSTS IN THE WESTERN EQUATORIAL PACIFIC, 1980-89

Leslie M. Hechtel
John A. Young

Dept. of Meteorology
University of Wisconsin - Madison
1225 West Dayton Street
Madison WI 53706

This Scientific Report presents some early results of research into the synoptic and dynamic structures leading to westerly wind bursts (WWBs) in the western equatorial Pacific. These bursts are potentially important as triggering mechanisms for ENSO events through the anomalous zonal stresses they place on the equatorial ocean. They also change the magnitude and distribution of air-sea fluxes in the western equatorial Pacific region. The plans for the 1992-93 TOGA (Tropical Ocean Global Atmosphere) COARE (Coupled Ocean-Atmosphere Response Experiment) field experiment include the possibility of measurements during a strong WWB event. This "quick-look" atlas is intended, in part, to assist in COARE planning.

We present estimated probabilities of WWBs exceeding 5 $m \cdot s^{-1}$ at different times of the year based on ECMWF (European Center for Medium-Range Weather Forecasts) analyses of 1000 mb wind (1980-1989). These figures clearly show the annual cycle of WWBs as well as some important intraseasonal variations in WWBs during high and low phases of the Southern Oscillation Index (SOI).

1. Data

This research was conducted using the ECMWF/WMO (World Meteorological Organization) data set. The basic data consists of twice-daily, 2.5° gridded, initialized fields of horizontal winds, omega, temperature, humidity, and geopotential heights at 1000, 850, 700, 500, 300, 200, and 100 mb. As with other assimilated data, it has the advantage of effective

space-time interpolation and the disadvantage of susceptability to model biases. We believe that it is adequate for identifying WWBs and their gross characteristics. This study uses only the zonal wind component at 1000 mb, a variable which is less sensitive to model or assimilation assumptions than many variables. As shown elsewhere (Young, 1990), the zonal wind component is a dominant part of the non-divergent tropical flow, and so it is less affected by initialization damping of the secondary circulation, while the 1000 mb wind is in the planetary boundary layer, which is represented by many high vertical modes which are not initialized. For details of the changes to and shortcomings of the ECMWF analyses, the reader is referred to Trenberth and Olson (1988a,b) and the references therein.

The ECMWF/WMO analyses are archived at the National Center for Atmospheric Research (NCAR) in a format designed to be used with the Community Climate Model (CCM) processor, designated PROC02C. The ECMWF data was originally on a 2.5° degree grid; Fourier transforms were used to convert this into CCM history tape format on a triangular T42 Gaussian grid (Trenberth and Olson, 1988a). The resulting data has gridpoints every 2.8125° in longitude, with a point at 180°; within 10 degrees of the equator, points are spaced at intervals of ~2.8° latitude, with a 2.8° interval centered on the equator. The NCAR CCM processor PROC02C was used to produce the derived fields used in this study.

This work also makes use of the Climate Analysis Center (CAC) Southern Oscillation Index (SOI). This is computed as follows: monthly anomalies of sea-level pressure with respect to the 1951-1980 means are computed for Tahiti and Darwin; these are then standardized with the mean annual standard deviation from each station. The differences between these standardized anomalies (Tahiti minus Darwin) are then computed, and in turn this difference is divided by the standard deviation of the difference time series (Kousky, 1991, personal communication). Values of the SOI obtained from V. Kousky at CAC are shown in Fig. A1; negative values of the SOI frequently correlate with ENSO events, eg. 1982-83, 1986-87.

The remaining figures in this report show the probability density estimates for the ten years 1980-89. These were computed using the twice-daily ECMWF analyses; the results will be referred to as "daily". The binary variable WWIND, defined as equal to 1 if $u_{1000} \geq 5$ m·s^{-1}

and 0 otherwise, was computed for each observation time except February 29 and December 31. The former was omitted for the sake of simplifying the process of computing 10-year statistics; the latter was omitted because of data-reading problems. The probability density function was constructed at each gridpoint at each date and time by summing all available WWIND over the decade and dividing by the number in the ensemble (in most cases, 10). In order to increase the sample size and reduce the dependence of the estimates upon individual events during this relatively short time period, we have created the 30-day running mean of the original twice-daily probabilities. This has the effect of decreasing the values and providing a smoother annual cycle of the estimated probabilities. The 30-day running mean was computed while taking into account the periodicity of the year's worth of probability density.

2. *Maps*

Figures 1, 2, and 3 show selected maps of this probability density, plotted over the domain 130° E to 170° W and 10° S to 10° N. The primary COARE domain is 140° E - 180° E, 10° S - 10° N, with a concentration of measurements in the intensive flux array (IFA) centered at 2° S, 155° E. The intensive observing period (IOP) for COARE is November 1992 to February 1993. All four COARE IOP months are included in the maps that follow. In all three figures the finely-dashed contour indicates 2% and the coarsely-dashed lines indicate 15%, 20%, etc. See figure legends for further details.

Examination of Fig. 1 points out several features of WWBs in the decade. The annual cycle is very visible; westerlies greater than 5 $m \cdot s^{-1}$ appear in the northern edge of the domain in July, become more likely in August, and spread in longitudinal extent in September. By November, these westerlies are most likely north of western New Guinea and eastward to near the dateline, centered roughly on the equator. December has dramatically increased WWB probabilities north of New Guinea, but westerlies east of the island are now most likely to be found near and a few degrees south of the equator. In January the increase and southward shift of probabilities continues, with probabilities strengthening to > 4% south of 3° S and

reaching > 8% in the eastern part of the domain. February and March see a decrease in likelihood of westerlies over and north of New Guinea, while westerlies over the ocean south of 2-3° S remain likely. In April the likelihood of westerlies diminishes greatly, and they are almost absent in May and June.

For COARE, this sequence indicates daily probabilities at the IFA to be near 2% for November, 4% in early December, 3% in January, and less than 2% in February. Higher probabilities are found to the southeast of the IFA in December, January, and February.

Figures 2 and 3 show maps of the conditional probability of WWIND for the decade 1980-89. These were constructed in the same manner as those in Fig. 1 except that summation was done for SOI < -1.0 (low) and SOI > 1.0 (high). Probabilities of westerlies are much higher in the low SOI months throughout the year; the most dramatic increase in probabilities occurs in the eastern part of the domain. Probabilities of westerlies are somewhat dimished to the west. Near-equatorial values greater than 4% persist near 170° E from June through December. The January values are quite large near the dateline at 7° S. The implications for the central COARE region during the low SOI phase are 5% probabilities for November and December, and less than 2% thereafter. In high SOI months, however, the probability of westerlies is quite low and is usually confined to the longitudes near New Guinea (130° E - 150° E). The December peak probabilities are less than 2% in the center of the COARE domain.

3. Longitude-Time Diagrams

The seasonal evolution of WWIND probabilities at any latitude is nicely summarized by the longitude-time ('Hovmoller') diagrams shown in Figure 4 and 5. We focus on latitudes within 7° of the equator, as these are most important to the oceanic waveguide (Harrison, 1989) and will be the site of the most intensive COARE observations. When looking at all latitudes for all years (Fig. 4), westerlies are seen to occur from June through December in the north, and progressively later further south, until at 7° S they have become a November through April phenomenon. In the low SOI case (Fig. 5), the basic march from north to south during June

through April remains as in the 'normal' case, but there is more activity to the east and less to the west, especially from 1.4° N to 4.2° S. In the Southern Hemisphere in low SOI years, westerlies are found almost year-round.

Probabilities for three Southern Hemisphere latitudes are shown in Fig. 4a and 5a. During all years at 1.4° S, a latitude of COARE emphasis, there is a clear December maximum west of 150° E, with a weaker secondary maximum eastward to 170° E. The main maximum decreases continuously through January and February. Further to the south, the entire COARE region experiences increasing probabilities during December, with a maximum lasting beyond February.

For low SOI conditions (Fig. 5a), the seasonal evolution near the equator (1.4° S) is very different, with maximum WWB probabilities near 170° E starting in July, reaching a peak in November, and abruptly ending by January. The low SOI probabilities at 4.2° S are characterized by an earlier start and eastward shift compared to the 'normal' pattern (Fig. 4a). The low SOI pattern is similar to the full pattern, but the probabilities are much higher.

The probability pattern for all years at 1.4° N (Fig. 4b) is similar to that at 1.4° S, with an early December maximum, except for the decline to less than 2% during January. Further north, probabilities are weaker and reach a maximum a few months earlier. Figure 5b shows that during low SOI years the seasonal evolution is very abnormal. At 1.4° N the primary maximum is in November between 160° E and 180° E. At 4.2° N that maximum occurs earlier, and at 7° N the activity dies during October, and is mainly west of 170° E.

References

Harrison, D.E., 1989: Local and remote forcing of ENSO ocean waveguide response. *J. Phys. Ocean.*, **19**, 692-695.

Trenberth, K.E. and J.G. Olson, 1988a: ECMWF global analyses 1979-1986: Circulation statistics and data evaluation. NCAR/TN-300+STR, 94 pp + fiche.

Trenberth, K.E. and J.G. Olson, 1988b: Intercomparison of NMC and ECMWF global analyses: 1980-1986. NCAR/TN-301+STR, 81 pp.

Young, J.A., 1990: Problems of surface wind assimilation for the tropical Pacific. Pages 3-13 in Air-Sea Interaction in the Tropical Western Pacific, Chao Jiping and John A.

Young, editors, China Ocean Press, Beijing.

Acknowledgements

This research was sponsored by NSF Grant ATM87-17255 to the University of Wisconsin-Madison. Some computations were done using the facilities at the National Center for Atmospheric Research (NCAR), which is sponsored by the National Science Foundation. Extensive use was also made of NCSA Telnet, developed at the National Center for Supercomputing Applications in Champaign, Illinois. The ECMWF analyses in NCAR CCM history-tape format are archived at NCAR, and were constructed from the original analyses by Jerry Olson and Kevin Trenberth.

FIGURE 1. Values of the "daily" probability of westerly winds ≥ 5 m·s^{-1} at 1000 mb for all years. Original twice-daily values have had a 30-day running mean applied; those shown are valid at 12 UTC.

a) day 10 = January 10
   day 40 = February 9
   day 70 = March 11

b) day 100 = April 10
   day 130 = May 10
   day 160 = June 9

c) day 190 = July 9
   day 220 = August 8
   day 250 = September 7

d) day 280 = October 7
   day 310 = November 6
   day 340 = December 6

Contour lines are as follows: finely dashed line = 2%; solid lines = 4, 6, 8, 10%; coarsely-dashed lines = 15, 20, 25%, etc.

Probability Density of WWIND, 1980-89

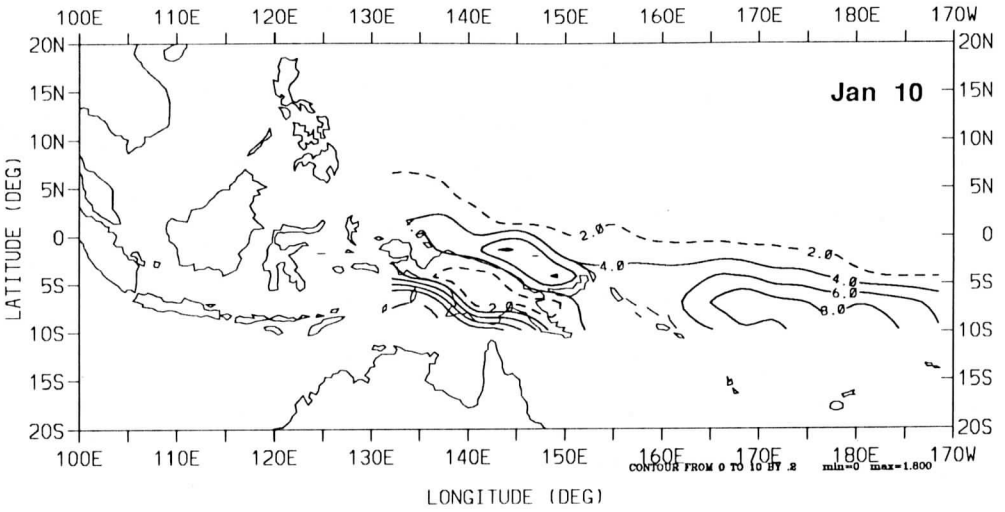

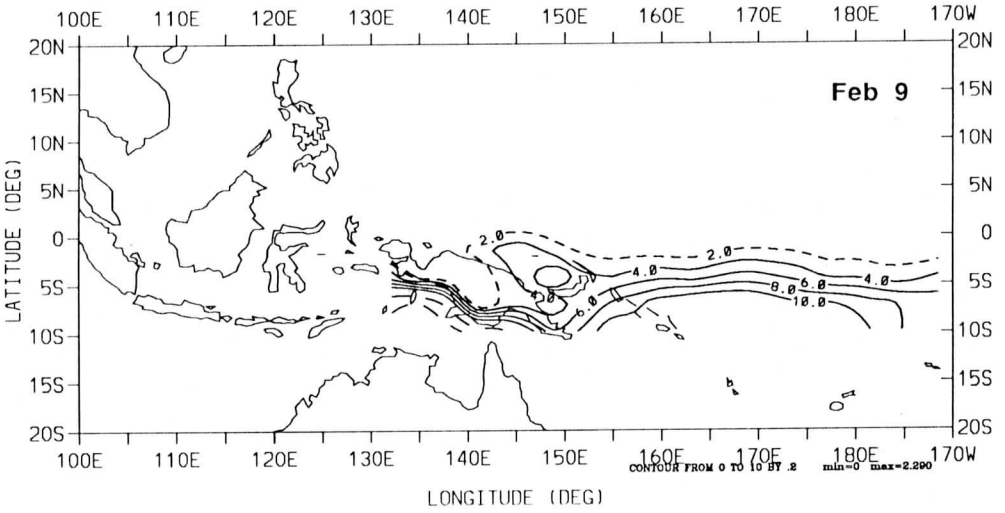

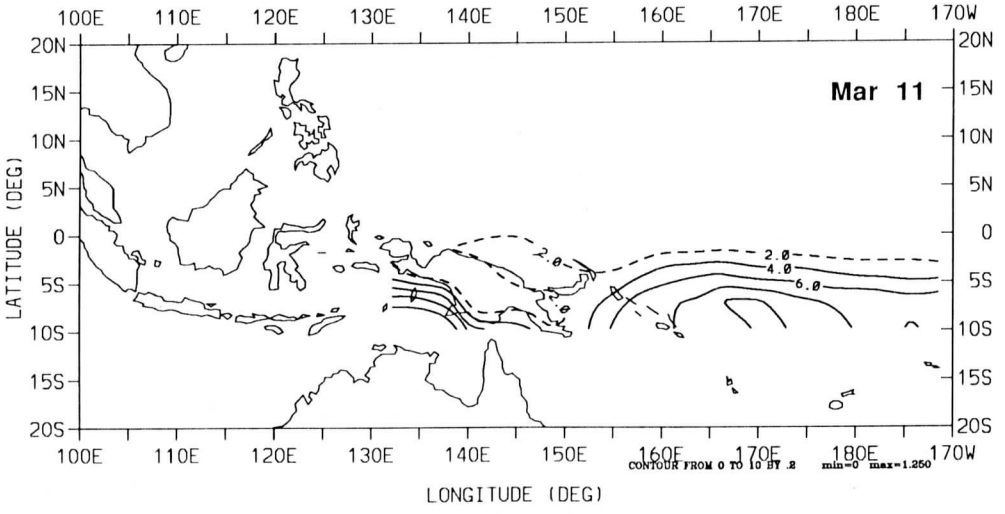

Probability Density of WWIND, 1980-89

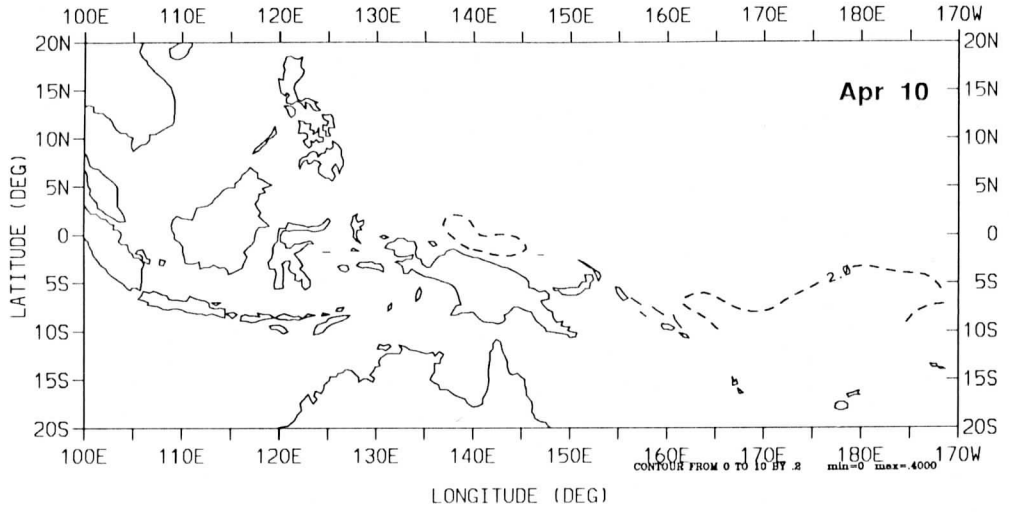

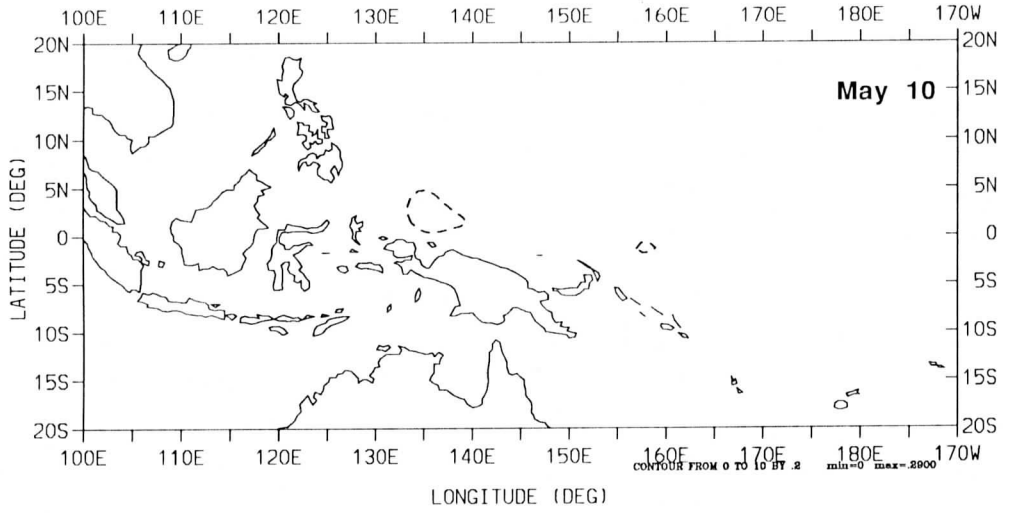

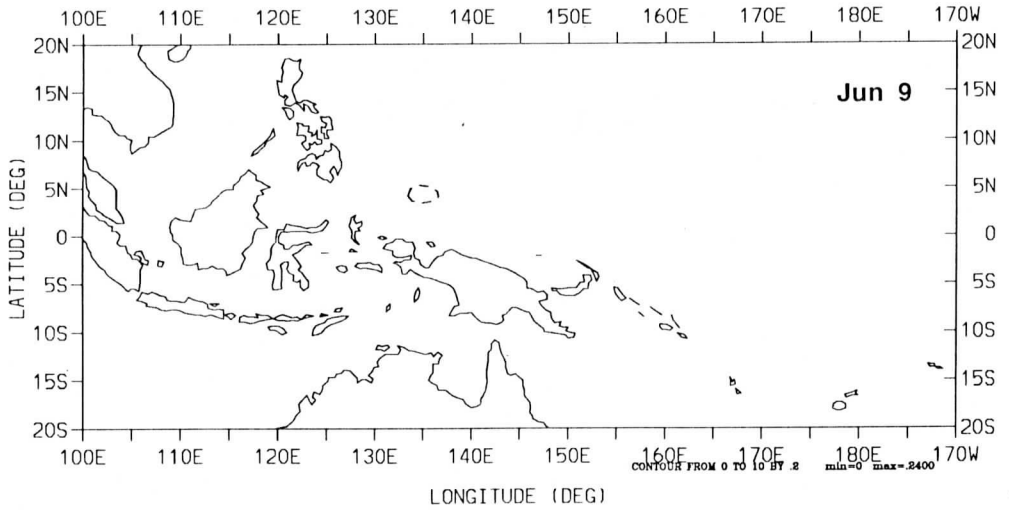

Probability Density of WWIND, 1980-89

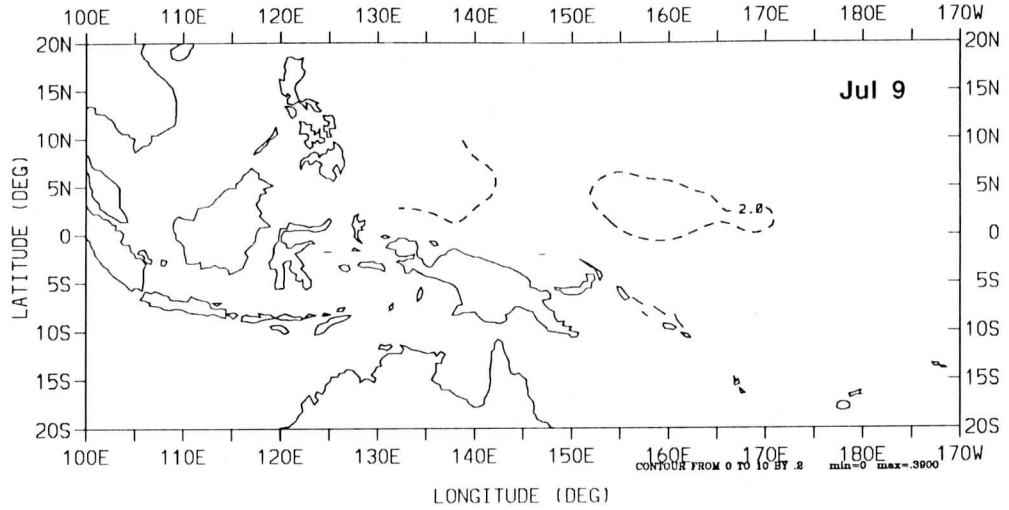

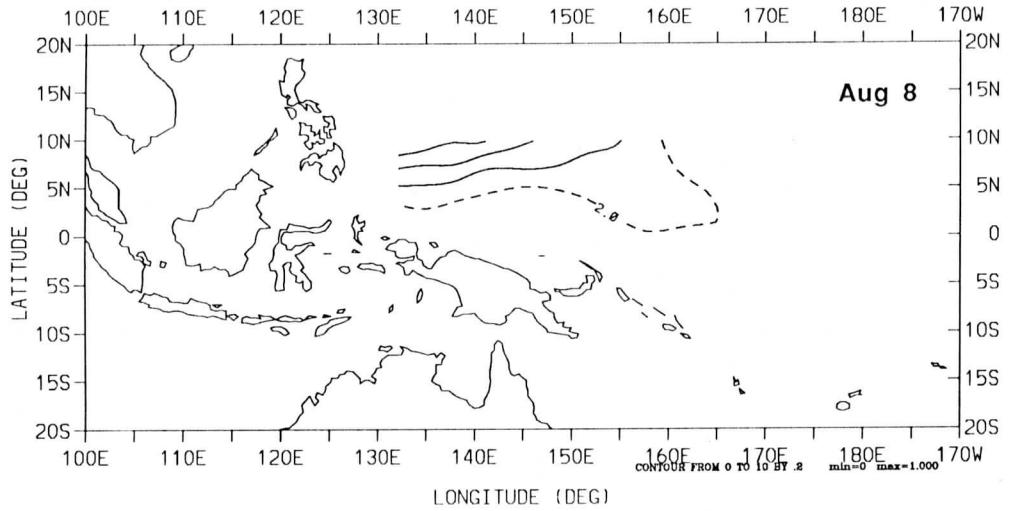

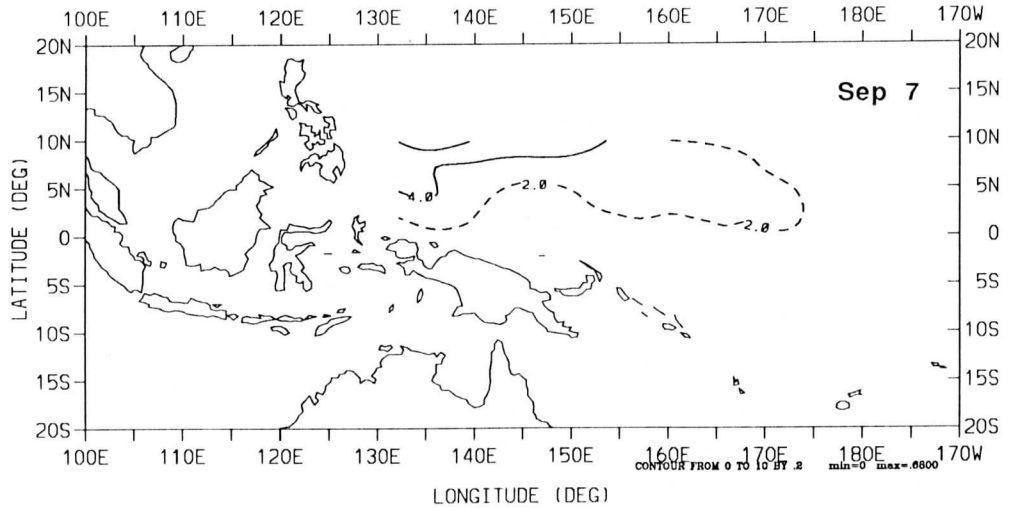

Probability Density of WWIND, 1980-89

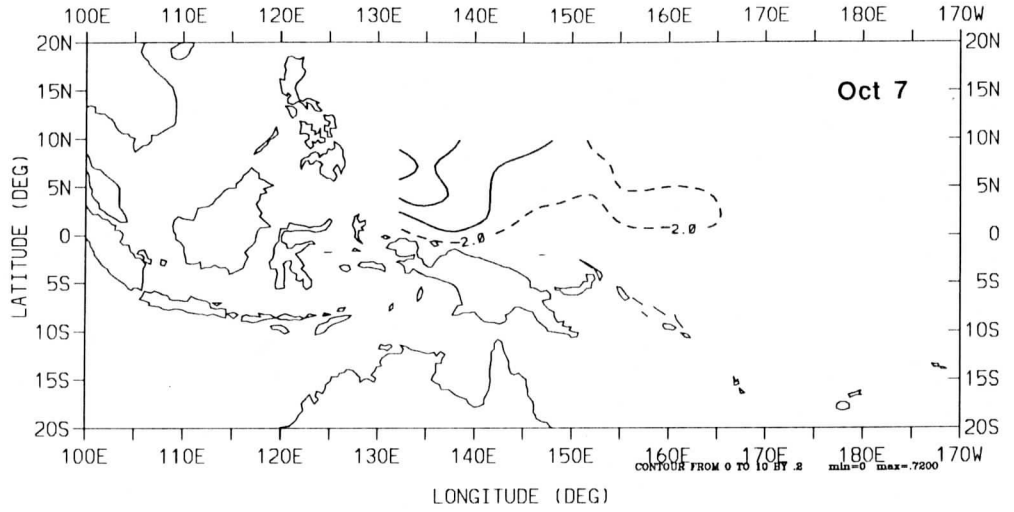

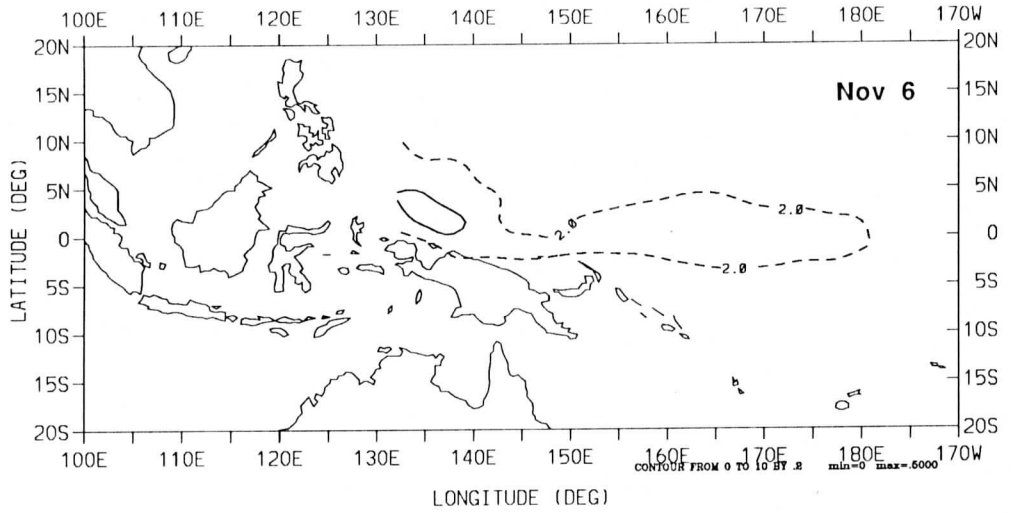

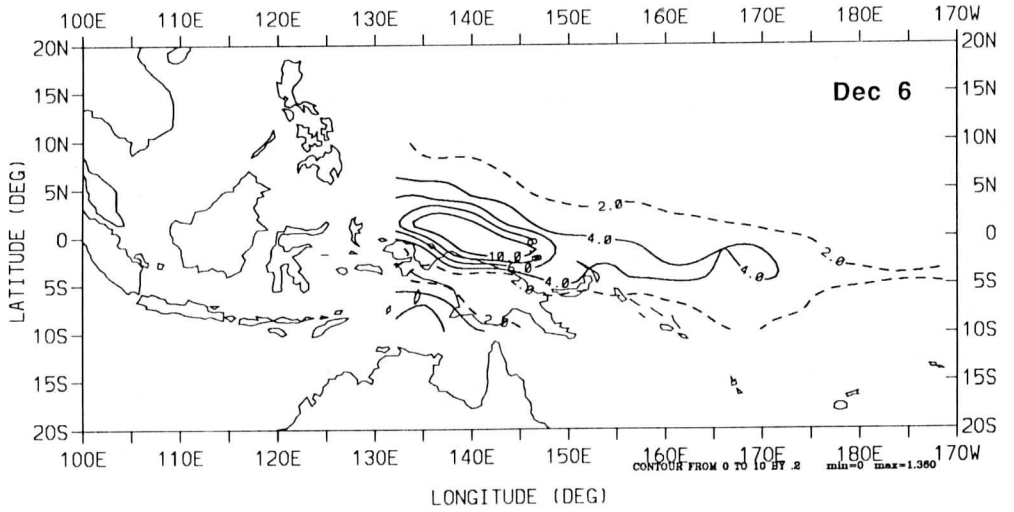

FIGURE 2. Values of the "daily" conditional probability of westerly winds ≥ 5 m·s^{-1} at 1000 mb for monthly SOI 'low', i.e. < 1.0. Original twice-daily values have had a 30-day running mean applied; those shown are valid at 12 UTC.

a) day 10 = January 10
   day 40 = February 9
   day 70 = March 11
b) day 100 = April 10
   day 130 = May 10
   day 160 = June 9
c) day 190 = July 9
   day 220 = August 8
   day 250 = September 7
d) day 280 = October 7
   day 310 = November 6
   day 340 = December 6

Contour lines are as follows: finely dashed line = 2%; solid lines = 5, 10%; coarsely-dashed lines = 15, 20, 25%, etc.

Probability Density of WWIND (SOI < -1.0), 1980-89

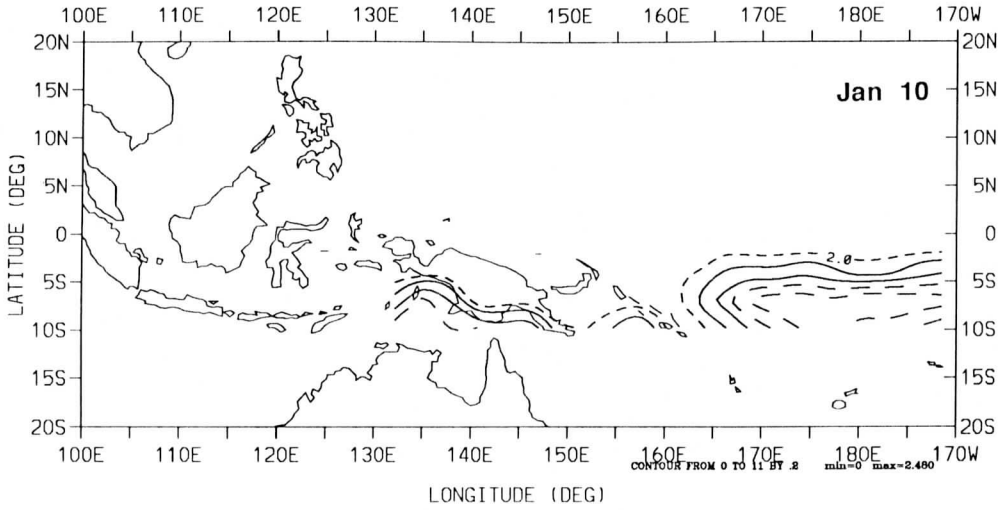

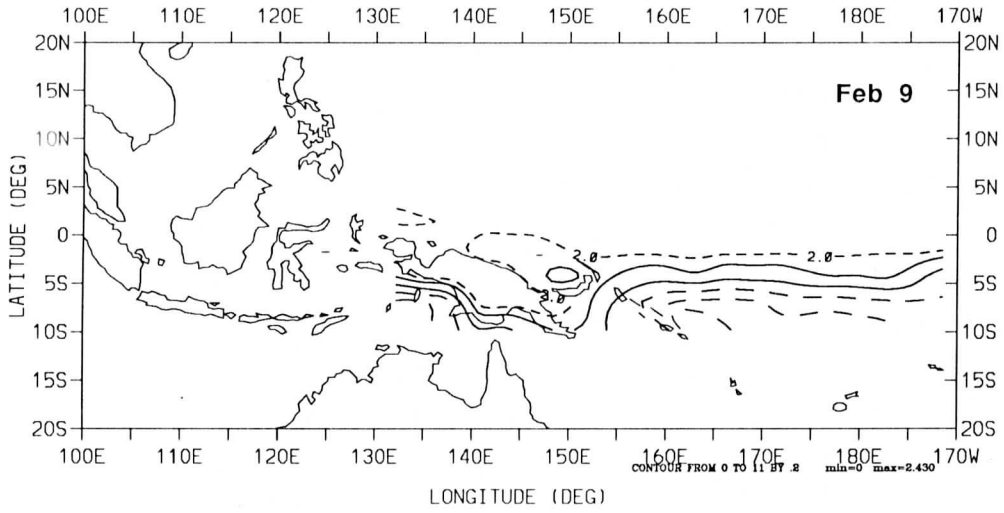

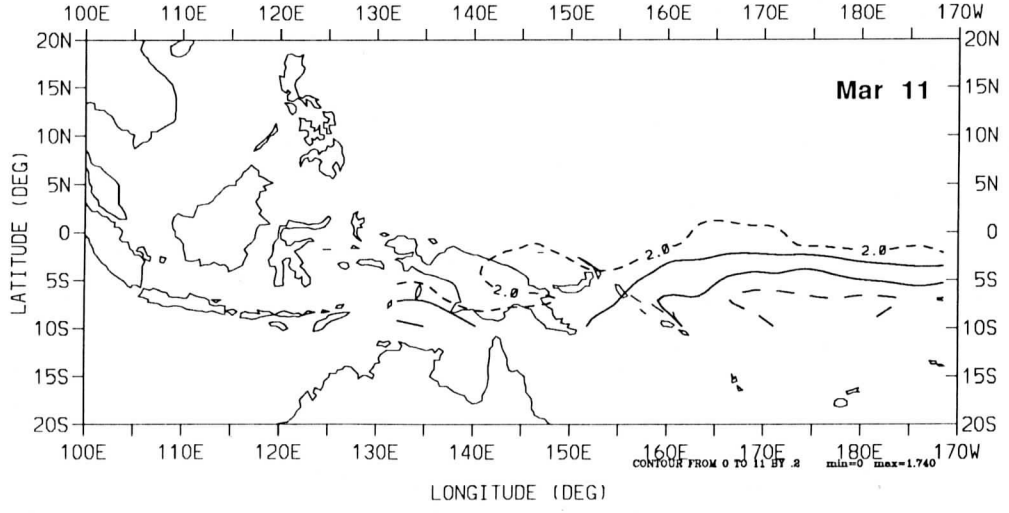

Probability Density of WWIND (SOI < -1.0), 1980-89

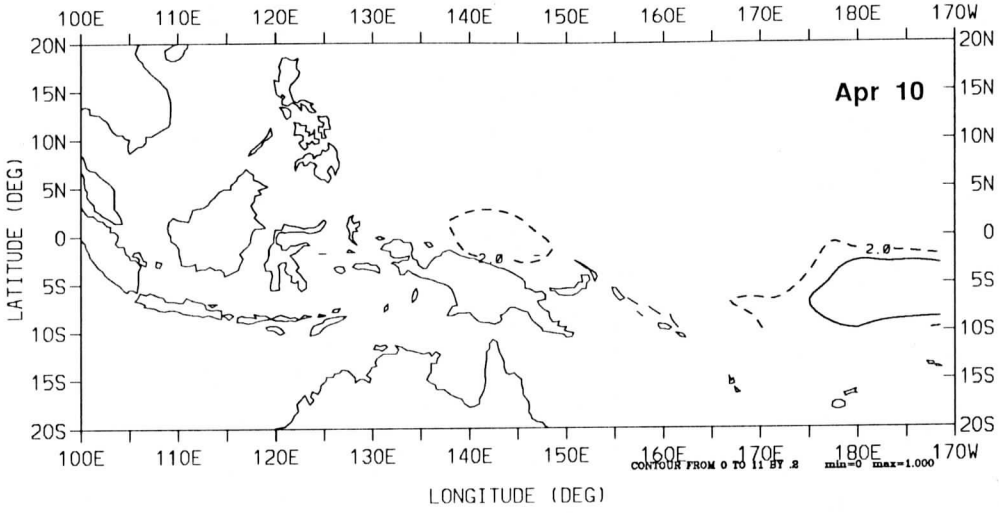

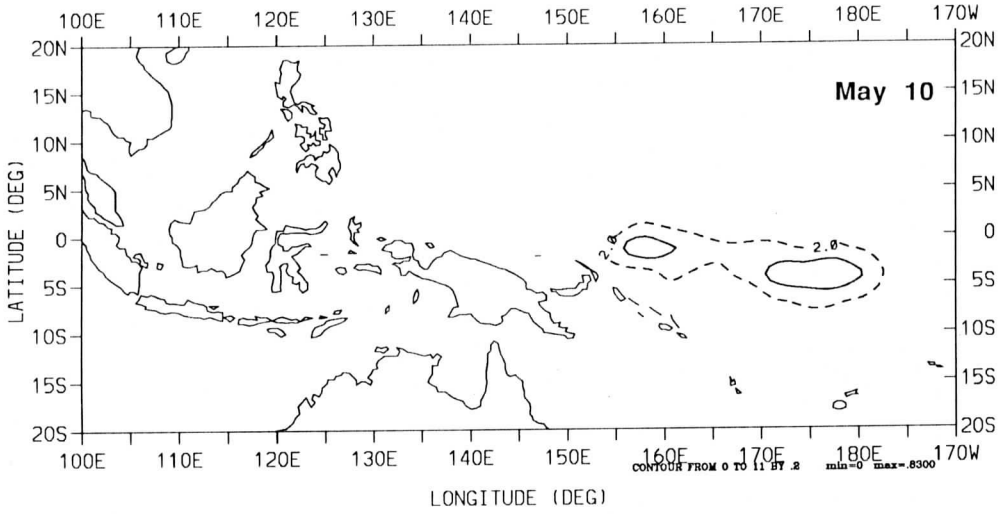

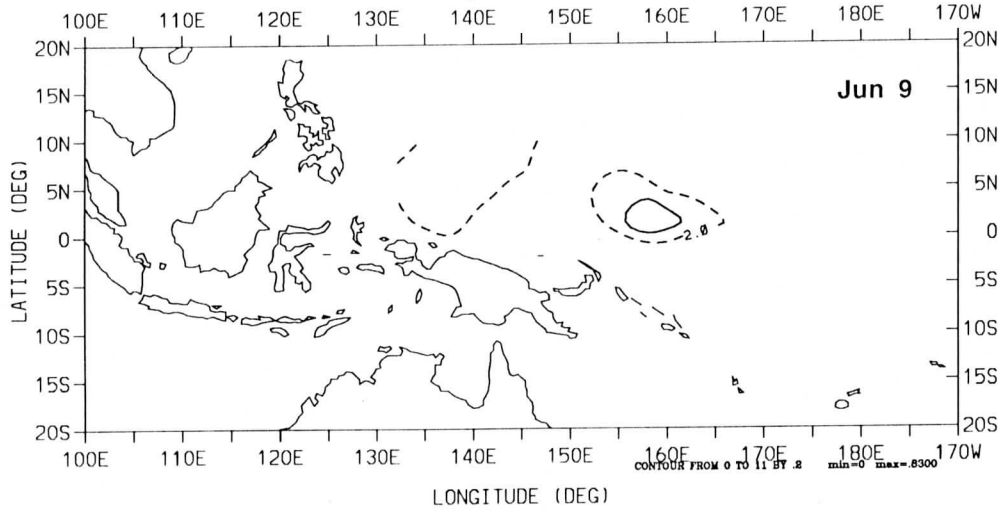

Probability Density of WWIND (SOI < -1.0), 1980-89

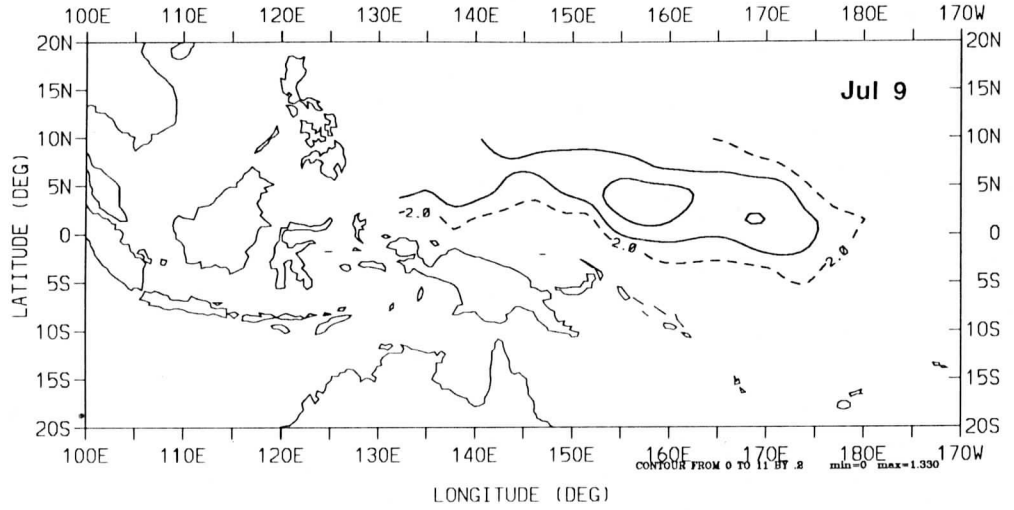

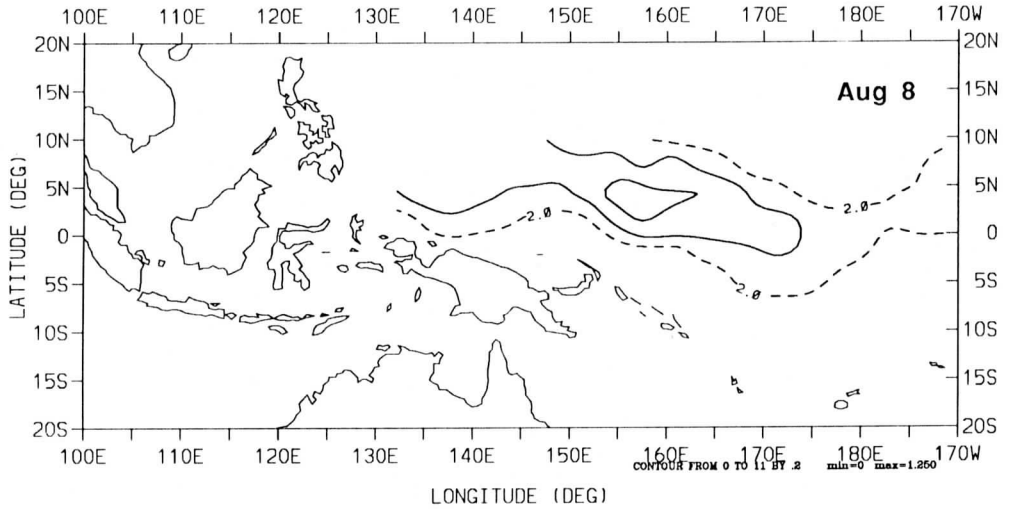

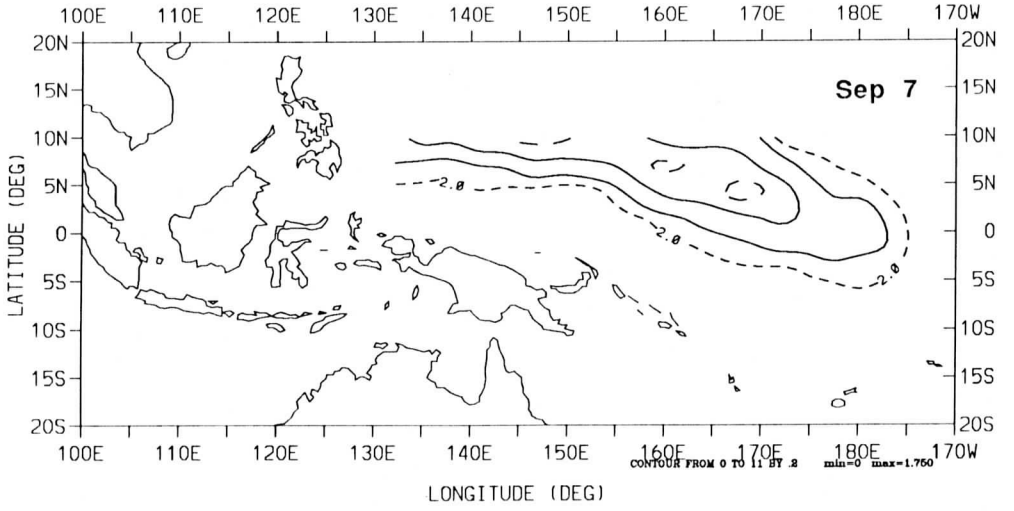

Probability Density of WWIND (SOI < -1.0), 1980-89

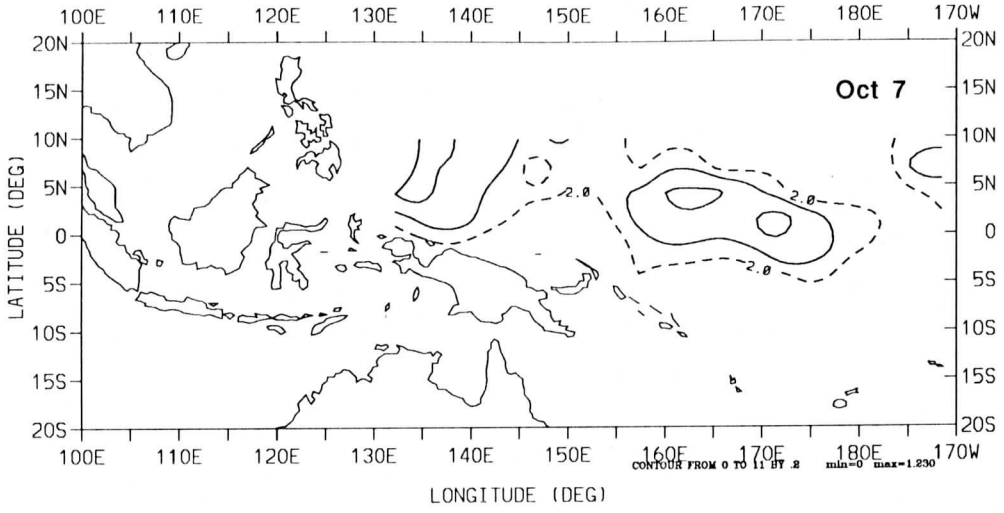

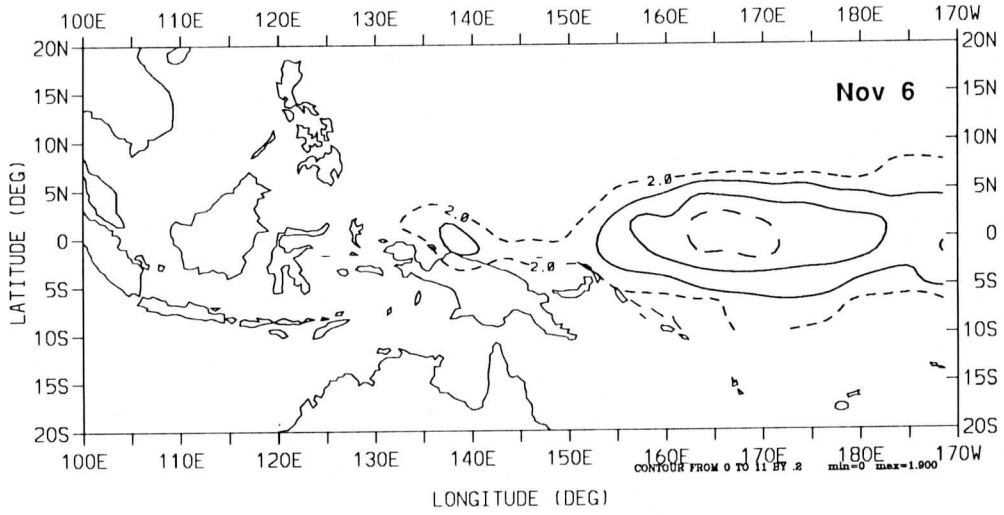

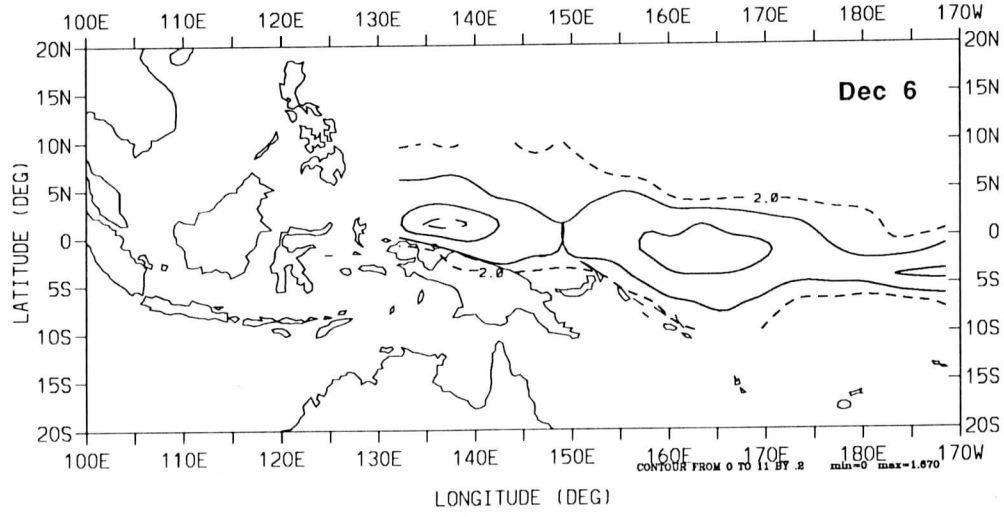

FIGURE 3. As in Figure 2 but for monthly SOI 'high', i.e. > 1.0.

a) day 10 = January 10
   day 40 = February 9
   day 70 = March 11
b) day 100 = April 10
   day 130 = May 10
   day 160 = June 9
c) day 190 = July 9
   day 220 = August 8
   day 250 = September 7
d) day 280 = October 7
   day 310 = November 6
   day 340 = December 6

Contour lines are as follows: finely dashed line = 2%; solid lines = 4, 6, 8, 10%; coarsely-dashed lines = 15, 20, 25%, etc.

Probability Density of WWIND (SOI > 1.0), 1980-89

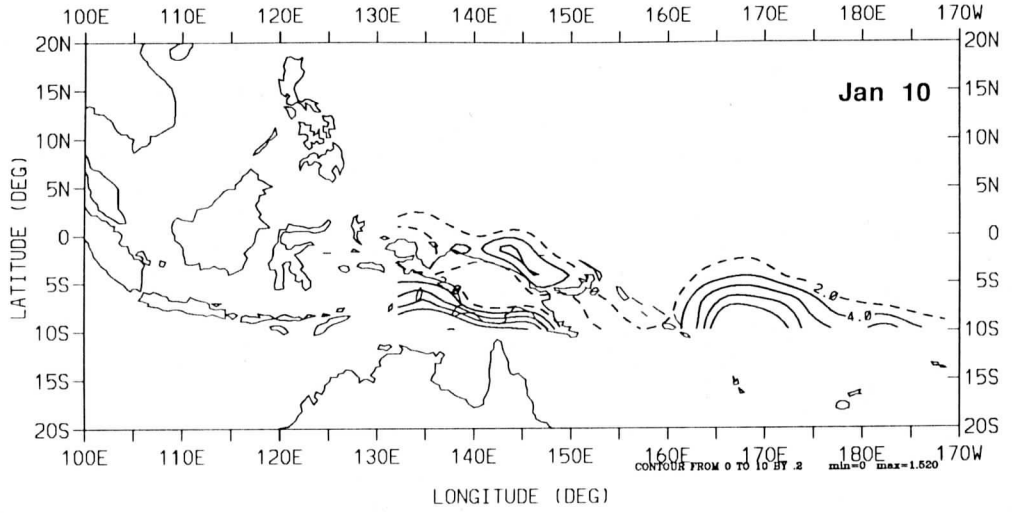

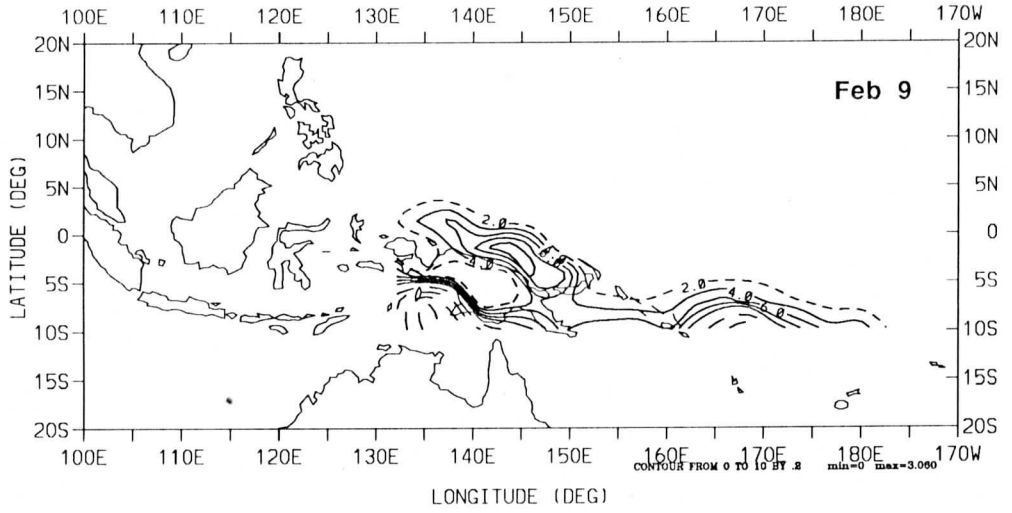

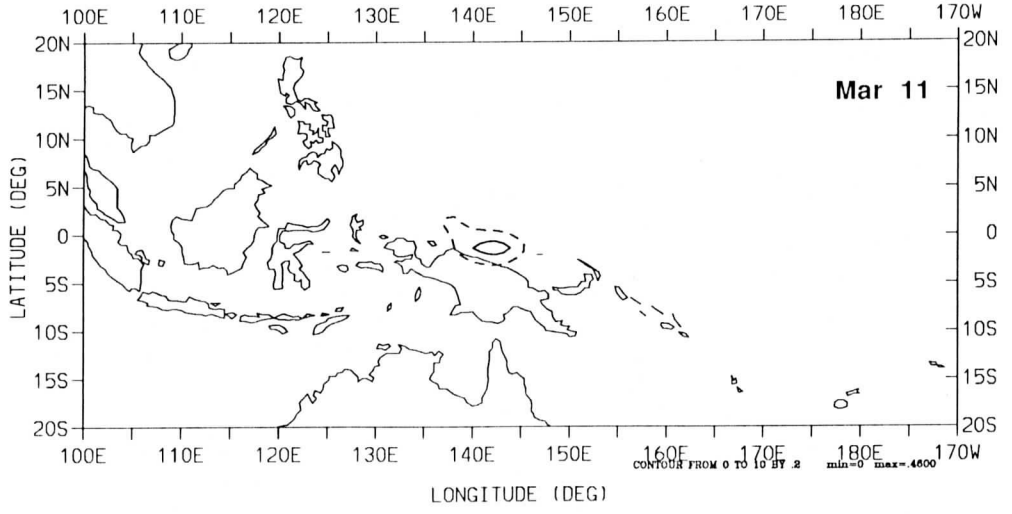

Probability Density of WWIND (SOI > 1.0), 1980-89

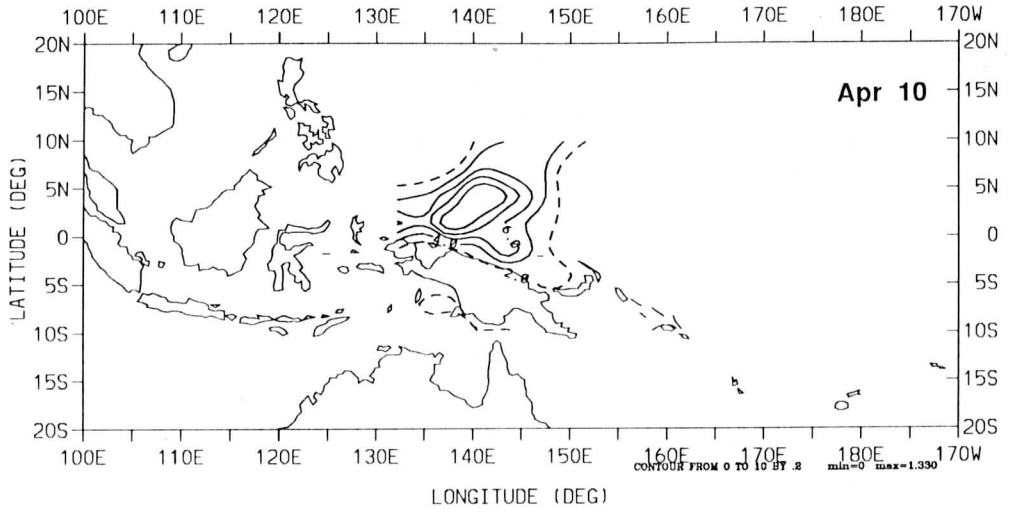

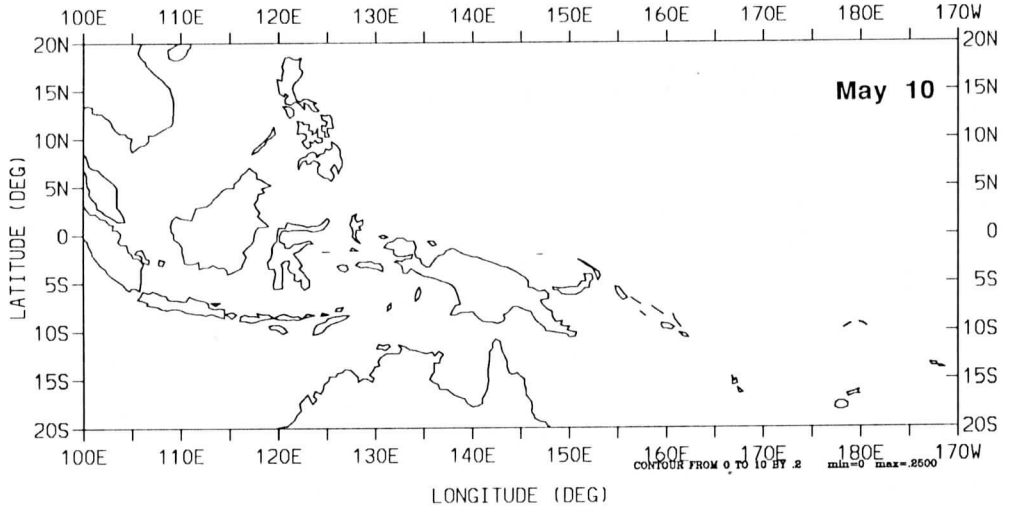

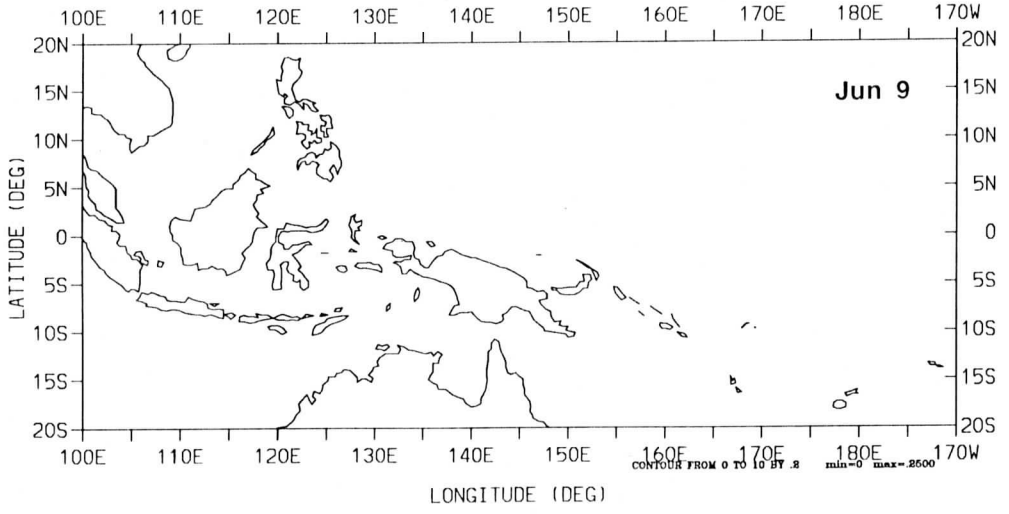

Probability Density of WWIND (SOI > 1.0), 1980-89

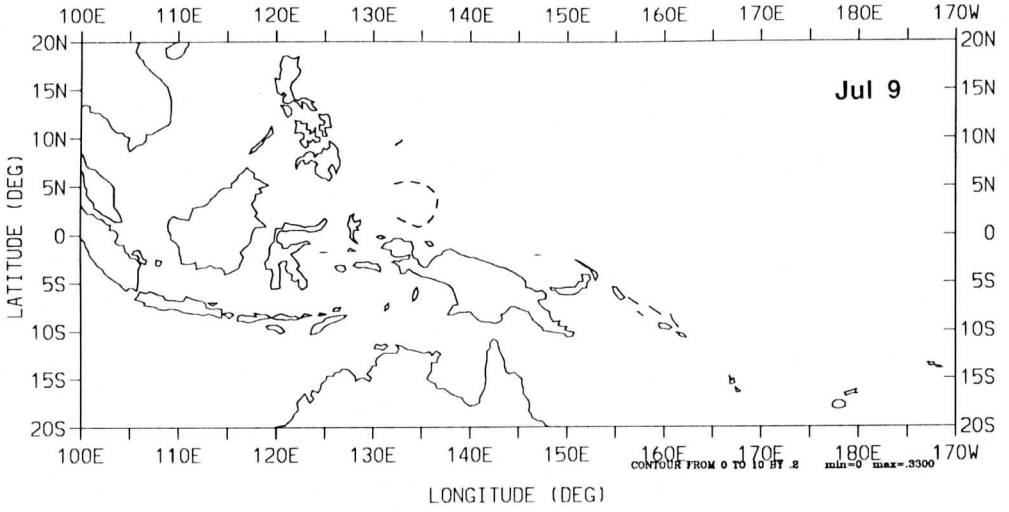

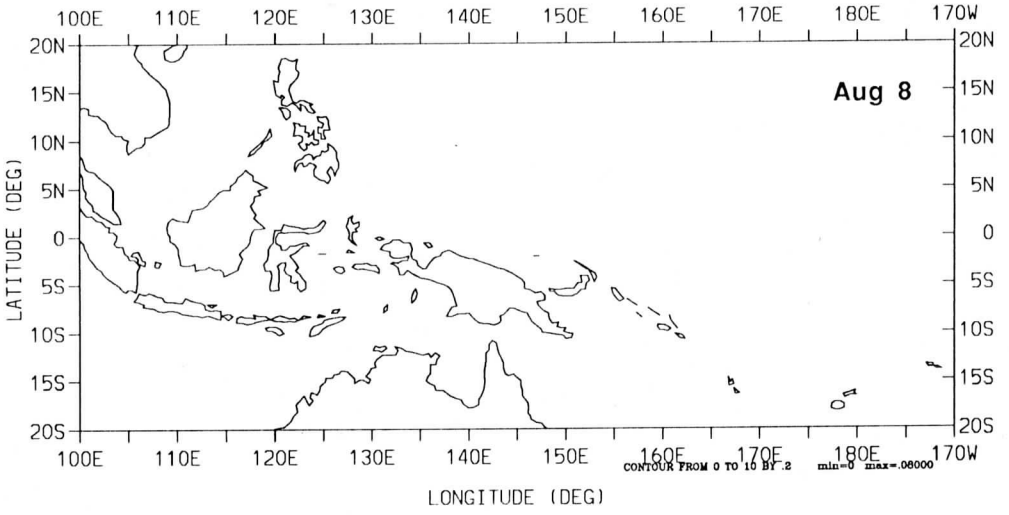

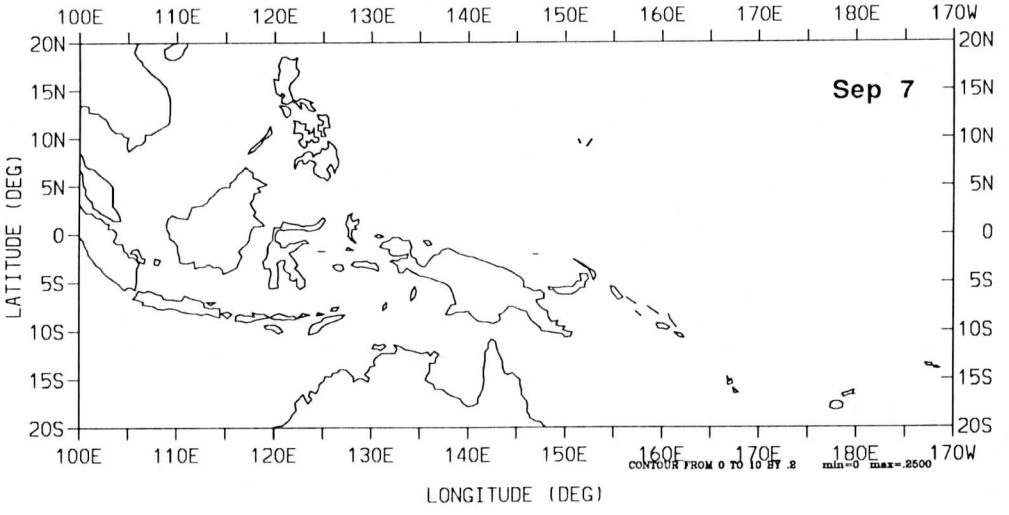

Probability Density of WWIND (SOI > 1.0), 1980-89

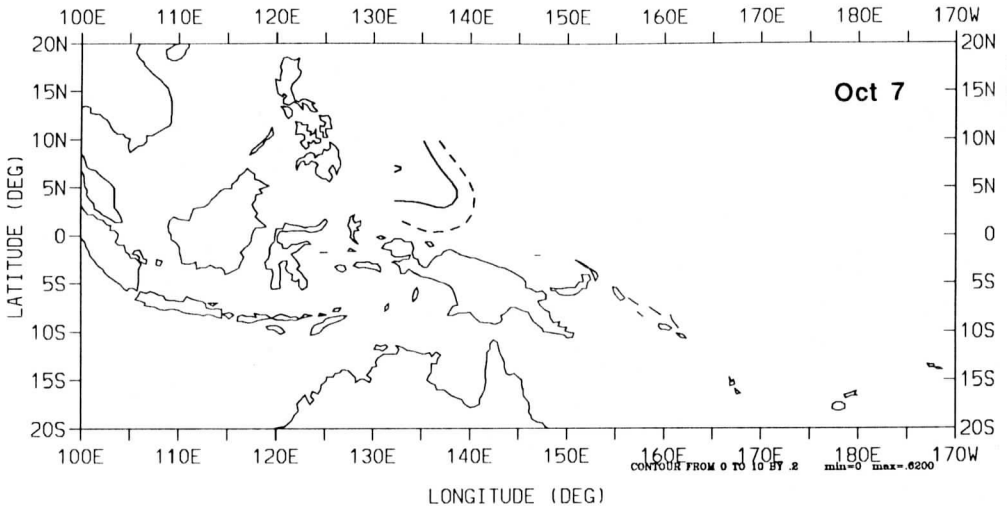

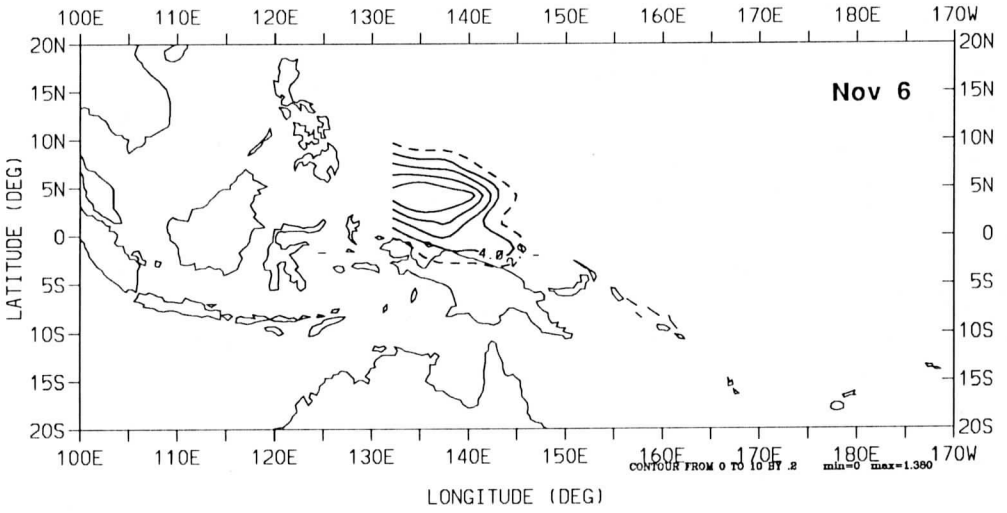

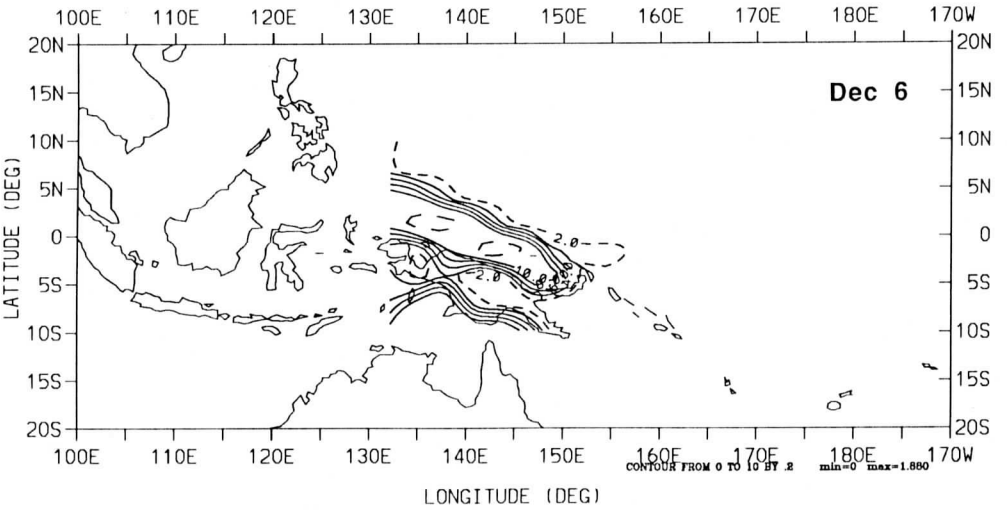

FIGURE 4. Longitude-time diagrams of the probability of westerly winds ≥ 5 m·s^{-1} at 1000 mb at several latitudes. Original twice-daily values have had a 30-day running mean applied. Note the year runs from July to June.

a) 7.0° S
   4.2° S
   1.4° S

b) 1.4° N
   4.2° N
   7.0° N

Contour lines are as follows: finely dashed line = 2%; solid lines = 4, 6, 8, 10%; coarsely-dashed lines = 15, 20, 25%, etc.

Probability Density of WWIND, 1980-89

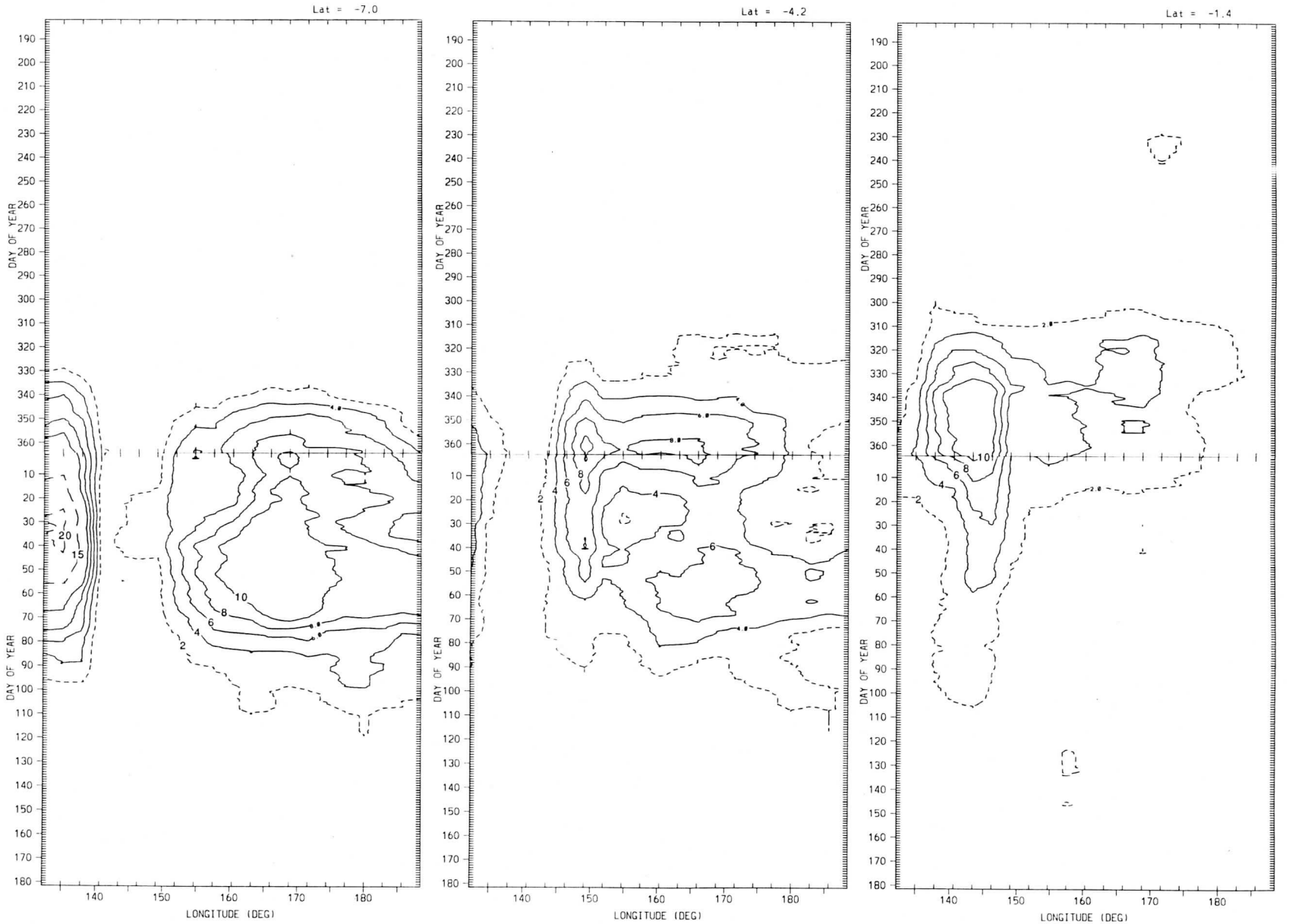

Probability Density of WWIND, 1980-89

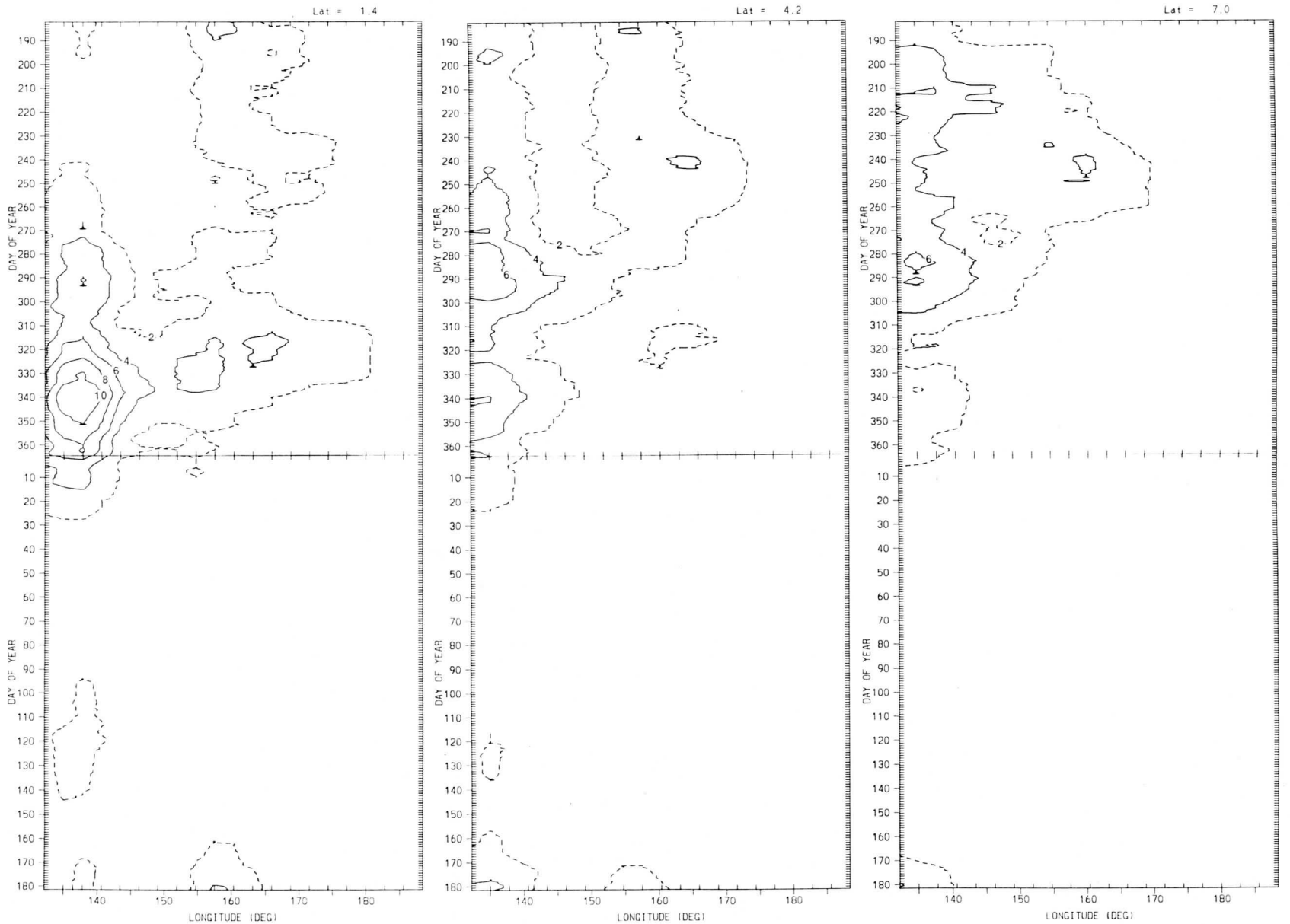

FIGURE 5. Longitude-time diagrams of the conditional probability of westerly winds ≥ 5 m·s^{-1} at 1000 mb for monthly SOI 'low', i.e. < 1.0, at several latitudes. Original twice-daily values have had a 30-day running mean applied. Note the year runs from July to June.

a) 7.0° S
   4.2° S
   1.4° S
b) 1.4° N
   4.2° N
   7.0° N

Contour lines are as follows: finely dashed line = 2%; solid lines = 5, 10%; coarsely-dashed lines = 15, 20, 25%, etc.

Probability Density of WWIND (SOI < -1.0), 1980-89

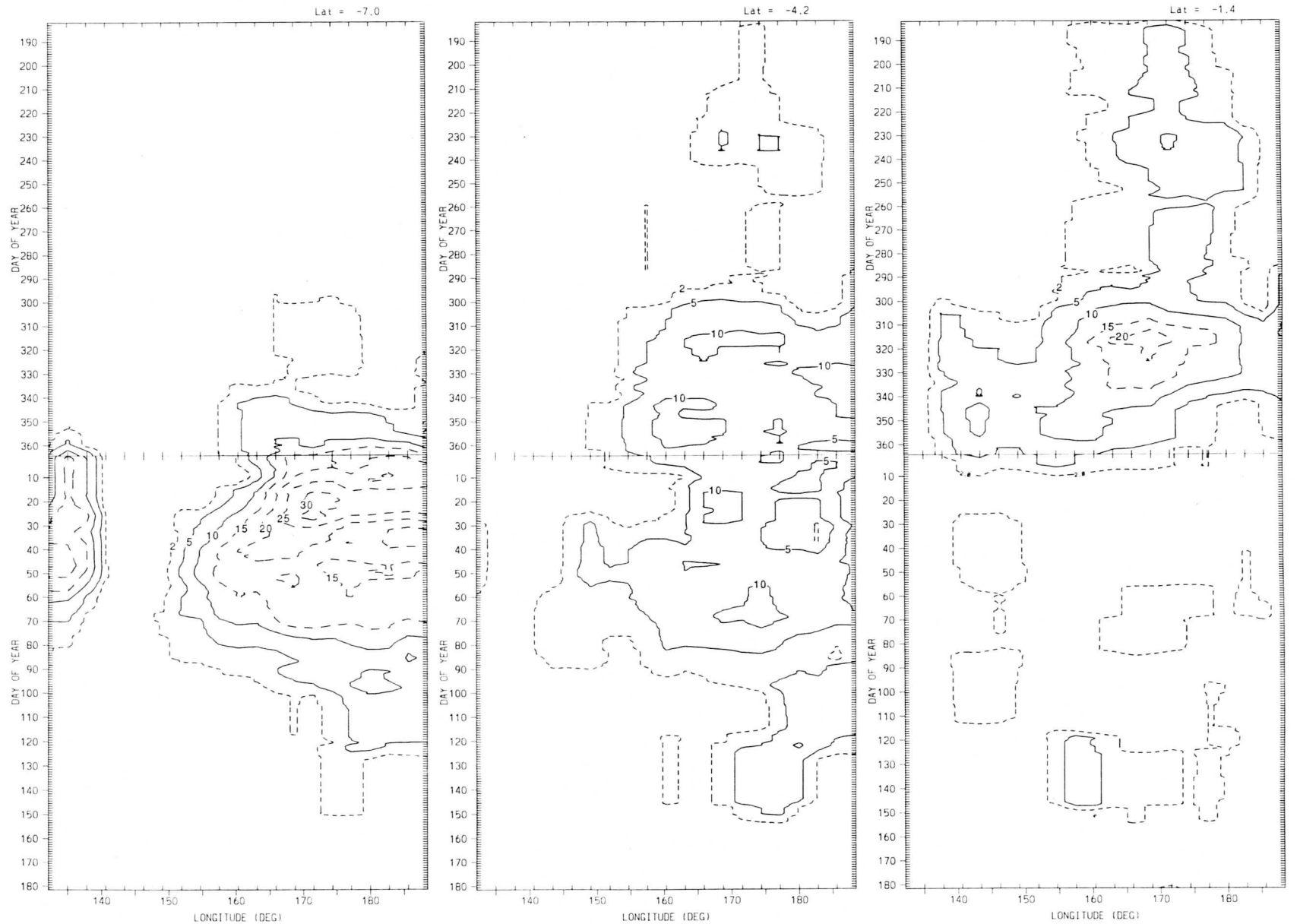

Probability Density of WWIND (SOI < -1.0), 1980-89

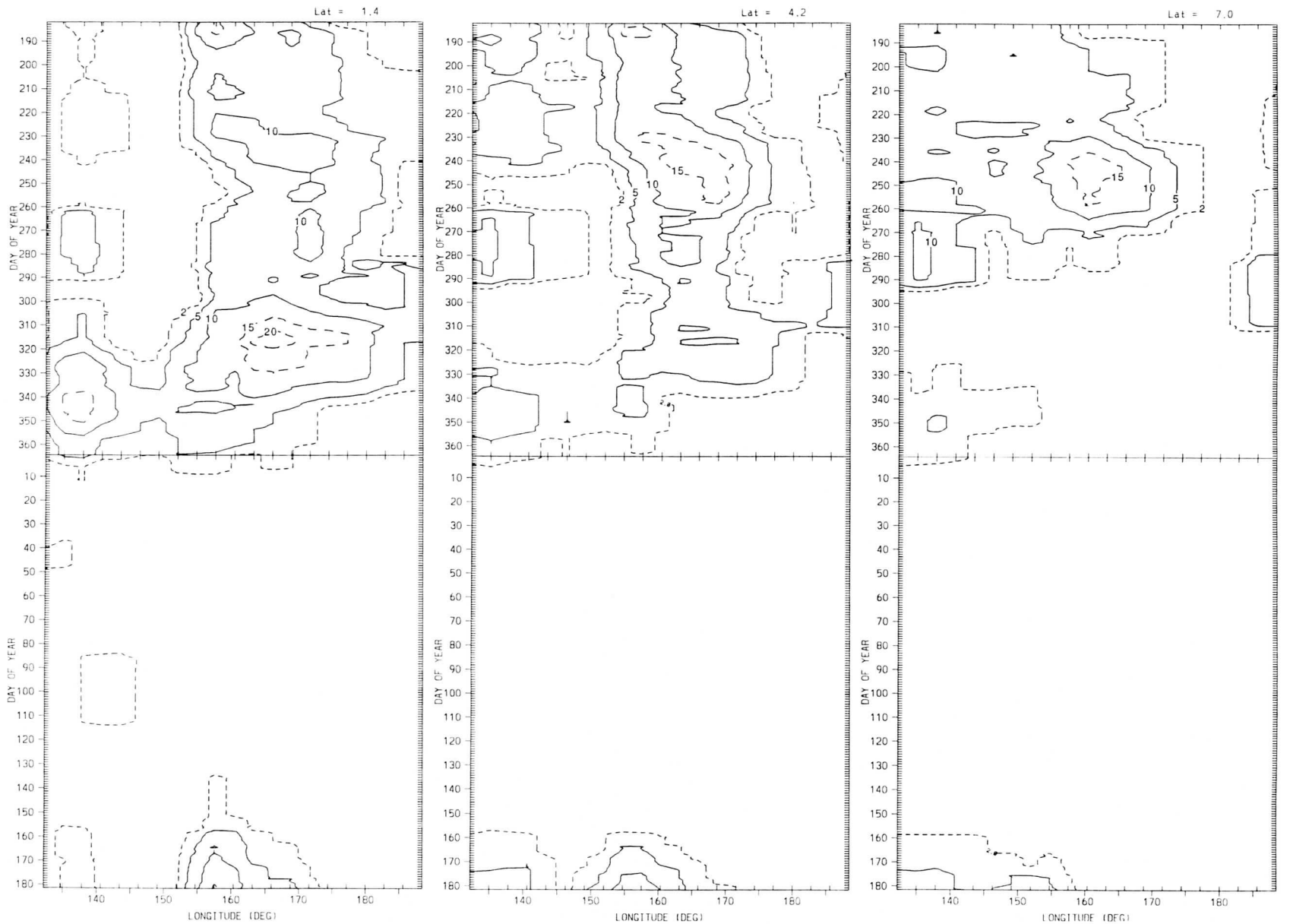

FIGURE A1. Monthly values of the Southern Oscillation Index (SOI) for the years 1980-1989. (V. Kousky, 1991, personal communication).

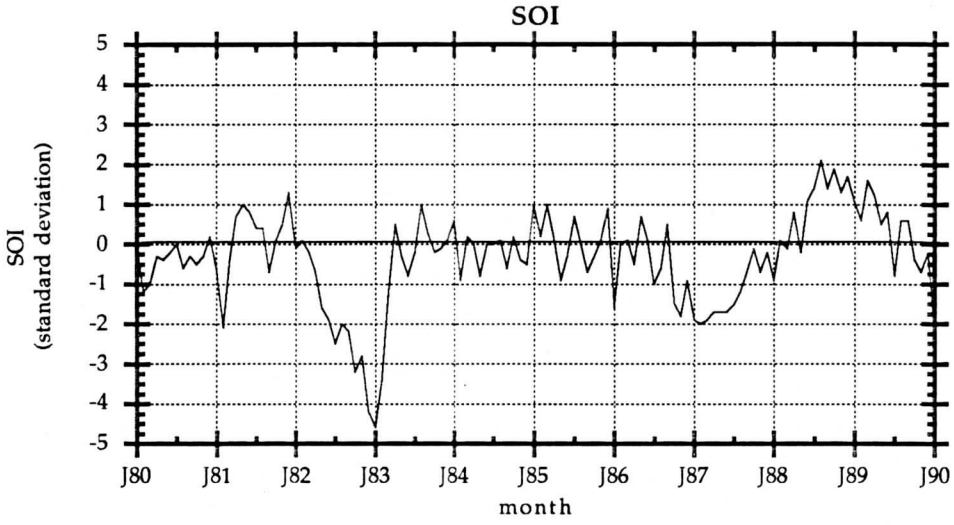
SOI
SOI
(standard deviation)
5
4
3
2
1
0
-1
-2
-3
-4
-5
J80
J81
J82
J83
J84
J85
J86
J87
J88
J89
J90
month